



This is a repository copy of *Strengthening of infilled reinforced concrete frames with TRM: Study on the development and testing of textile-based anchors.*

White Rose Research Online URL for this paper:  
<http://eprints.whiterose.ac.uk/99976/>

Version: Accepted Version

---

**Article:**

Koutas, L. [orcid.org/0000-0002-7259-6910](http://orcid.org/0000-0002-7259-6910), Pitytzogia, A., Triantafillou, T.C. et al. (1 more author) (2013) Strengthening of infilled reinforced concrete frames with TRM: Study on the development and testing of textile-based anchors. *Journal of Composites for Construction*, 18 (3). ISSN 1090-0268

[https://doi.org/10.1061/\(ASCE\)CC.1943-5614.0000390](https://doi.org/10.1061/(ASCE)CC.1943-5614.0000390)

---

**Reuse**

Unless indicated otherwise, fulltext items are protected by copyright with all rights reserved. The copyright exception in section 29 of the Copyright, Designs and Patents Act 1988 allows the making of a single copy solely for the purpose of non-commercial research or private study within the limits of fair dealing. The publisher or other rights-holder may allow further reproduction and re-use of this version - refer to the White Rose Research Online record for this item. Where records identify the publisher as the copyright holder, users can verify any specific terms of use on the publisher's website.

**Takedown**

If you consider content in White Rose Research Online to be in breach of UK law, please notify us by emailing [eprints@whiterose.ac.uk](mailto:eprints@whiterose.ac.uk) including the URL of the record and the reason for the withdrawal request.



[eprints@whiterose.ac.uk](mailto:eprints@whiterose.ac.uk)  
<https://eprints.whiterose.ac.uk/>

**This is the version of the paper submitted to ASCE after peer review and prior to copyediting or other ASCE production activities.**

**You can find the final, copyedited (online) version of the published paper here:**  
[http://ascelibrary.org/doi/abs/10.1061/\(ASCE\)CC.1943-5614.0000390](http://ascelibrary.org/doi/abs/10.1061/(ASCE)CC.1943-5614.0000390)

**You can cite this paper as:**

Koutas, L., Pitytzogia, A., Triantafillou, T., and Bousias, S. (2013). "Strengthening of Infilled Reinforced Concrete Frames with TRM: Study on the Development and Testing of Textile-Based Anchors." *J. Compos. Constr.*, 10.1061/(ASCE)CC.1943-5614.0000390, A4013015.

## **Strengthening of Infilled Reinforced Concrete Frames with TRM: Study on the Development and Testing of Textile-based Anchors**

L. Koutas<sup>1</sup>, A. Pitytzogia<sup>2</sup>, T. C. Triantafillou, M. ASCE<sup>3</sup> and S. N. Bousias, M. ASCE<sup>4</sup>

### **Abstract:**

The paper presents a technique for strengthening of reinforced concrete infilled frames with textile-reinforced mortar (TRM) jacketing. Key objective of the study is to examine different methods of masonry infill-concrete connection by developing and testing textile-based anchors at the interface between masonry wallettes and concrete. The parameters examined include mainly the type of boundary conditions at the masonry-concrete interface, the geometry and fiber volume of anchors and the type and number of layers of the textile. It is shown that the anchors developed in this study enable the transfer of substantial tensile forces between masonry and concrete, and that their magnitude may be estimated on the basis of anchor properties.

**CE Database subject headings:** masonry infills; reinforced concrete; seismic retrofitting; strengthening; textile anchors; textile-reinforced mortar (TRM).

---

<sup>1</sup> Post-graduate student, Dept. of Civil Engrg., Univ. of Patras, Patras GR-26500, Greece.

Email: koutasciv@upatras.gr

<sup>2</sup> Post-graduate student, Dept. of Civil Engrg., Univ. of Patras, Patras GR-26500, Greece.

<sup>3</sup> Professor, Dept. of Civil Engrg., Univ. of Patras, Patras GR-26500, Greece.

Email: ttriant@upatras.gr

<sup>4</sup> Associate Professor, Dept. of Civil Engrg., Univ. of Patras, Patras GR-26500, Greece.

Email: sbousias@upatras.gr

## Introduction and Background

It is widely accepted that the contribution of masonry infills in the seismic performance of reinforced concrete (RC) structures is significant in cases that they do not cause adverse effects, such as shear failure of columns. The increase in the lateral load resistance and the additional energy dissipation are some of the beneficial characteristics offered by infills, due to their interaction with the members of the surrounding RC frame. Key feature of the infill-RC frame interaction after significant lateral deformation has developed is the formation of a strut in one diagonal of the infill panel and the separation of the infill from the frame at the two opposite corners in the other diagonal. Failure of masonry infills during this interaction is typically brittle, as a result of masonry cracking and/or crushing.

Strengthening of the masonry infills in order to achieve a better performance during seismic loading is a rational solution, which gains increasing popularity. The conventional strengthening technique of masonry infills comprises the application of external steel-mesh reinforcement on the face of the infill in combination with shotcrete or plaster (e.g. [Altin et al. 2010](#)). Alternative strengthening techniques found in the literature are based on the application of sprayable ductile-fiber reinforced cementitious composites (e.g. Kyriakides and Billington 2008), steel fiber reinforced mortars (e.g. [Sevil et al. 2011](#)) and fiber-reinforced polymer (FRP) sheets.

The use of FRP materials for strengthening of masonry infills in RC frames has been experimentally investigated in a number of studies during the last decade and has been proved to be effective in terms of both lateral resistance and energy dissipation. In particular, this strengthening technique has been used for: (i) strengthening single storey – single bay infilled frames using carbon FRP (CFRP) sheets applied onto the entire masonry surface ([Saatcioglu et al. 2005](#)), glass FRP (GFRP) strips laid horizontally ([Almusallam and Al-Salloum 2007](#)) or CFRP strips placed diagonally ([Altin et al. 2008](#), [Erol et al. 2008](#), [Nateghi-Elahi and Dehghani 2008](#)); (ii) strengthening two storey – single bay infilled frames via diagonally

placed CFRP strips (Ozcebe et al. 2003, [Yuksel et al. 2006](#), Akin et al. 2009, Ozden et al. 2011); and (iii) strengthening the middle infilled bay of a two storey – three bay frame (Erdem et al. 2006).

In an attempt to alleviate some problems associated with FRP, especially with regards to epoxy resins, researchers have introduced the concept of combining advanced fibers in the form of textiles with inorganic matrices, e.g. cement-based mortars. The so-called textile-reinforced mortars (TRM) have been reported as an extremely promising solution in many cases of seismic retrofitting RC structures. In particular, TRM has been used for the: confinement of concrete (Triantafillou et al. 2006) and RC columns with or without lap-splices ([Bournas et al. 2007](#), Bousias et al. 2007, [Bournas et al. 2009](#), Bournas and Triantafillou 2011); shear strengthening of RC beams (Triantafillou and Papanicolaou 2006, Brückner et al. 2008, Blanksvärt et al. 2009, [Al-Salloum et al. 2012](#)); flexural strengthening of RC beams (Triantafillou 2007, Elsanadedy et al. 2013); flexural strengthening of two-way RC slabs (Papanicolaou et al. 2009); and strengthening of RC beam-column joints ([Al-Salloum et al. 2011](#)). TRM have been used quite successfully also as strengthening materials for unreinforced masonry walls subjected to out-of-plane ([Papanicolaou et al. 2008](#), Harajli et al. 2010) or in-plane (Papanicolaou et al. 2007, [Parisi et al. 2011](#)) loading.

In the present study, the TRM strengthening technique is extended one step further; it is applied for the first time in the field of masonry infill walls. The concept is described in the next section, which is followed by an experimental study on newly developed anchors to be used in combination with TRM at masonry infill-concrete interfaces.

### **Strengthening of Infilled Reinforced Concrete Frames with Textile-Reinforced Mortar (TRM)**

The concept proposed herein considers strengthening of unreinforced masonry infills in seismically deficient reinforced concrete structures via TRM. The basic idea lies in converting

a masonry infill from a brittle element that fails in the early stages of a strong ground motion, into a reliable load-carrying element with favorable infill - surrounding frame interaction characteristics. Thus, except for applying the layers of TRM on the infill surfaces, the proper connection between the infill and the elements of the surrounding frame is also desired. This connection needs to be done in a way guaranteeing the transfer of tensile forces between masonry and concrete.

Key objective of the present study is to examine methods of infill-frame connection for two different cases of boundary conditions, as follows (Fig. 1a):

(i) The thickness of the masonry infill is less than the width of the concrete frame elements. In this case there is a step at the boundary, hence simple extension of the TRM layers from the masonry to the concrete surface is not feasible and the transfer of forces from concrete to masonry has to be achieved through the use of anchors (e.g. left column or bottom slab in Fig. 1b).

(ii) The thickness of the masonry infill is equal to the width of the concrete frame elements. In this case the TRM layers can be extended to the concrete surface up to a length that is practically feasible, on both sides of the infill. If the element of the surrounding frame is a T-beam, the TRM layers can be extended up to the slab and possibly anchored there (top slab in Fig. 1b), while if the concrete element is a rectangular column, the TRM layers can cover the two faces of the column or even be wrapped around, if possible (right column in Fig. 1a, b). Moreover, if the adjacent frame bay is infilled and the boundary has the same conditions, the TRM layers can be extended to the adjacent infill.

If the thickness of the infill is not equal to the width of the bounding concrete element and the infill is placed eccentrically, it is possible that the two sides of the infilled frame have different infill-frame boundary conditions, so that both (i) and (ii) described above apply, one on each side.

The two aforementioned cases were simulated experimentally by constructing and testing two types of specimens (Fig. 2), each one representing a part of the infill anchored to an adjacent concrete element through an anchor. The specimens shown in Fig. 2a and Fig. 2b correspond to the above cases (i) and (ii), respectively. The specimens were subjected to tension, in order to simulate separation between infills and the surrounding concrete frame and the development of tension forces in the anchors placed through the infill-concrete interface.

## **Experimental Program**

### ***Test Specimens and Experimental Parameters***

The experimental program aimed at studying the behavior of new textile-based anchors as tension elements between TRM-strengthened brick wallettes and reinforced concrete prisms. A total of 19 specimens were fabricated and split in two series, each one representing a different case of frame-infill boundary conditions.

In order to examine the case of an existing step between the infill and the concrete element of the surrounding frame, six specimens with the geometry shown in Fig. 2a were constructed (Series A). Each specimen of this series consisted of a 200x200x300 mm reinforced concrete prism and a 400x400 mm brick wallette with a thickness of 85 mm. Because the main objective of this series was to examine the capacity of the anchors in transferring tensile forces directly from the brick wallette to the RC prism, the parameters under investigation were the quantity of fibers in the anchors and the depth at which the anchors were inserted in the concrete. The brick wallette of each specimen was strengthened on both sides with one layer of a glass-fiber textile combined with a commercial polymer-modified cement mortar.

The case of infills with thickness equal to that of surrounding concrete elements was investigated through 13 specimens with the geometry shown in Fig. 2b (Series B). Each specimen of this series consisted of a T-shaped reinforced concrete prism and a brick wallette. The specimens of this series were designed such that the role of several parameters on the effectiveness of this strengthening technique could be investigated, namely: the type of textile used as externally bonded reinforcement on each side of the brick wallette, the number of layers of the textile, the quantity of fibers in the anchors, the length of the anchors on the infill and the orientation of the part of the anchors placed inside the concrete. Details of the material properties as well as a description of the strengthening procedures are given in the next section.

All specimens tested are summarized in Table 1 and are shown schematically in Fig. 3. The notation given to the specimens of Series A is  $A\_WX-DY_I$ , where:

- A stands for Series A.
- X denotes the width of the textile which was used to form the anchor, in mm (W400 or W600 for a 400 mm and a 600 mm wide textile, respectively).
- Y denotes the depth of the hole in the concrete in which the straight part of the anchor was placed, in mm (D150 or D75 for a 150 mm and a 75 mm depth, respectively).
- The subscript  $I$  denotes the index (a or b) of twin specimens.

The notation of all specimens in Series B, except for the control ones, follows the format  $B\_TN\_WX-LY_I$ . Control specimens, that is specimens without anchors, are given the notation  $B\_TN\_CON$ . In this notation format:

- B stands for Series B.
- T denotes the type of textile used for the layers of the externally applied reinforcement (H or L for heavier or lighter textile, respectively).
- N denotes the number of layers (1 or 2).
- CON stands for control specimens.

- X denotes the width of the textile which was used to form the anchor, in mm (W400 or W600 for a 400 mm and a 600 mm wide textile, respectively), as in Series A.
- Y denotes the fan length, that is the length of the anchors at their part not embedded inside the concrete, in mm (L350 and L500 for 350 mm and 500 mm length, respectively).
- The subscript <sub>1</sub> denotes additional information: “in” for anchors placed inclined in the concrete and “eql” for replacement of anchors with an equivalent – in terms of volume of fibers in the direction of loading – layer of textile, on each side). It is noted that for the specimens without subscript <sub>1</sub> the anchors were placed nearly vertical in the holes. The depth of holes in this series of specimens was 100 mm.

### **Materials and Strengthening Procedures**

The reinforced concrete prisms were cast in three groups on different dates (Specimens 1-6, 7-10 and 11-19 of Table 1). As the concrete strength was not a parameter under investigation, no special measures were taken to achieve the same strength in all specimens. The average compressive strength at an age of 28 days (approximately equal to the age on the day of testing) measured on 150 mm cubes (average values from three specimens) is given in Table 2.

As in the case of reinforced concrete prisms, the wallettes were built in three groups on different dates (Specimens 1-6, 7-10 and 11-19 of Table 1). All the wallettes were constructed using perforated, fired clay bricks (190x85x55 mm), with the perforations running parallel to the unit's length. The thickness of the bed and the head mortar joints was approximately 10 mm. The mean compressive strength of the bricks perpendicular to the perforations was obtained from three compression tests, in which the bearing surfaces of the bricks were capped using a self-leveling, rapid-hardening cement mortar; the value obtained was equal to 4.4 MPa. The cement:lime:sand proportions in the mortar used to bind the bricks of the

wallettes was different for the three groups described above. Note that as masonry mortar strength was not a parameter under investigation, no special measures were taken to design the same mortar in all specimens.

For the first group of wallettes (Specimens 1-6) the above proportions were 1:0.5:4, whereas for the other two groups the proportions were the same and equal to 1:2:5. The strength of the mortar was obtained through flexural and compression tests, according to EN-1015-11 (1993). The flexural strength of the mortar was obtained from three-point bending on 40x40x160 mm prisms, whereas the compressive strength was obtained from compression tests of the fractured parts of the prisms used in flexural tests. The bearing surface of these parts was equal to 40x40 mm. The values of compressive and flexural strength (average values from three specimens) of the mortar used in this study are summarized in Table 3.

Two different textiles were used as externally bonded reinforcement of the specimens. For all the six specimens of Series A and four specimens of Series B (specimens 7-10) a commercial textile with equal quantity of epoxy-coated E-glass fibers in two orthogonal directions was used (hereafter mentioned as textile H – Fig. 4a). The mesh size and the weight of that textile were 10x10 mm and 610 g/m<sup>2</sup>, respectively. For the rest of the specimens (11-19) a lighter commercial textile (with a larger mesh size) made of elastomeric polymer-coated E-glass with equal quantity of fibers in two orthogonal directions was used (hereafter mentioned as textile L – Fig. 4b). The mesh size and the weight of that textile were 25x25 mm and 405 g/m<sup>2</sup>, respectively.

The anchors developed in this study were custom-made from a commercial textile made of uncoated basalt fiber rovings knitted in two orthogonal directions with equal quantity of fibers in each one (Fig. 4c). The mesh size and the weight of that textile were 25x25 mm and 192 g/m<sup>2</sup>, respectively. The reason for selecting this textile for the anchors was the requirement for an easy to unknit textile, so that the anchors could be produced with minimal

effort. The properties of all the textiles are summarized in Table 4, as given by the manufacturers or derived analytically where full data were not available.

The mortar used as a binding material between the textile and the substrate was a commercial fiber-reinforced cement-based mortar mixed with re-dispersible polymers. Strength properties were obtained through flexural and compressive testing, as in the case of the mortar used for the construction of brick wallets. The mean values of flexural and compressive strength at an age of 28 days were 4.7 MPa and 22.3 MPa, respectively and were the same for all the specimens (as the water to cementitious material ratio by weight was kept constant and equal to 0.2).

The anchors were based on the concept of “spikes”, often used in the case of FRP (e.g. Zhang and Smith 2012, Koutas and Triantafillou 2013). The procedure that was followed to form the anchors and prepare them for use on the day of the strengthening is described next. Initially, a part of the basalt textile was cut in the desired dimensions. The width of the textile was equal to either 400 mm or 600 mm and the length was equal to the depth of the hole in which the anchor would be inserted, plus the desired length of the fan that would be shaped at the end of the procedure (350 mm or 500 mm). The second step involved the removal of a certain number of fiber rovings in the direction parallel to the width of the textile (Fig. 5a). This step was necessary in order to form a tow of fibers at one end of the anchor. This tow had a length greater than the depth of the hole in which the anchor would be inserted by about 50 mm. As the main objective of this procedure was to create a textile-based anchor with a fanned part that could be easily applied over a TRM layer and have good bonding conditions, it was important to retain the grid of the textile at the fanned part and to ensure the alignment of the fiber rovings that would be activated in tension. A way to achieve that was by cutting the fiber rovings in the direction parallel to the height of the textile at certain distances (every two or three vertical rovings), thus creating separate grid parts (Fig. 5b). At this stage the anchor comprised a tow of fibers at one end and separate textile grids that could shape a fan at

the remaining part (Fig. 5c). The final step of this procedure was the impregnation with epoxy resin both of the fibers of the tow (Fig. 5d) and of the textile grids (Fig. 5e), followed by a subsequent period of two days for curing. Impregnation of the tow fibers facilitates the insertion of that part of the anchor into the predrilled hole in the concrete. Impregnation of the textile grids provides a stable and easy-to-apply material and increases the stiffness of the fiber rovings, thereby creating better conditions for the mechanical interlock between the textile and the mortar. It is important to note that the tow of fibers at one end of the anchor was impregnated only in a length equal to the depth of the hole, leaving a small portion in the central region of the anchor with dry fibers (Fig. 5f); these were impregnated with epoxy adhesive at a later stage, during the strengthening procedure. Within the framework of this study, the angle of the shaped fan of the anchors was not a parameter under investigation. Taking into consideration the geometric characteristics of all the specimens, this angle was made equal to 45°.

The application of textile layers and textile-anchors comprised the following steps: (a) drilling holes into the concrete prisms with a diameter of 12 mm and varying depth according to specimen design; (b) removing the dust from the holes and from the surfaces receiving the TRM layers with high air pressure; (c) application of protection to the holes in order to keep them dry and clean during the application of TRM layers; (d) dampening of the surfaces receiving mortar; (e) application of a thin layer of masonry mortar at the joint between the concrete prism and the brick wallette; (f) placement of the wallette on the concrete prism while the masonry mortar at the joint was in a fresh state; (g) application of mortar on both sides of the wallette (and the web of the concrete prism for specimens of Series B – Fig. 6a); (h) bonding of the textile by hand pressure (Fig. 6b); (i) application of mortar at the location of the fanned part of the anchor; (j) filling of the holes with low viscosity epoxy resin; (k) local impregnation of the dry fibers of the anchors with epoxy adhesive (Fig. 6c); (l) placement of the anchors into the holes, bonding of the fan over the first textile layer by hand

pressure and application of mortar on the top of the fan area (Fig. 6d); and (m) application of mortar in between the layers (in case of two layers), while the first layer was in a fresh state, as well as on the top of the last layer. The thickness of each layer was approximately 3 mm, thus resulting in a jacket with thickness of approximately 6 mm on each side of the specimens. At the location of the fan the total thickness was increased by approximately 2 mm.

In the case of control specimens, steps (a)-(c) and (i)-(l) were omitted. For specimen B\_L1\_W400-L500<sub>eq1</sub>, the procedure was the same as that for the control specimens, employing the basalt textile as a second textile layer. Finally, it should be mentioned that the TRM layers were applied to the entire brick wallette surface, except for the case of specimens B\_H1\_CON, B\_H1\_W400-L350 and B\_H1\_W400-L350<sub>in</sub> (see Fig. 3), where the TRM was applied only in the central region of the wallettes, at a width equal to that of the concrete prisms.

The adhesive used to fill the holes and to impregnate the fibers of the anchors during the anchor fabrication stage was a commercial, low viscosity, two-part epoxy resin with tensile strength and elastic modulus equal to 72.4 MPa and 3.2 GPa, respectively (values taken from the manufacturer data sheets). The adhesive used for the impregnation of the dry fibers central area of the anchors during the strengthening procedure was a special type commercial, low viscosity, two-part epoxy resin, which can be hardened under high humidity conditions, as those in the fresh mortar of the TRM system. The tensile strength and the elastic modulus of this adhesive were equal to 20 MPa and 3 GPa, respectively (values taken from the manufacturer data sheets).

In order to obtain experimental values for the tensile strength of the basalt fibers after impregnation with epoxy resin, three epoxy impregnated basalt fiber tows were tested in tension. The fiber tows were formed from a 200 mm wide basalt textile (the one used for the anchors) after removing all transversal fiber rovings. A mean tensile strength of 15.5 kN was

obtained from the three tests (14.3 kN, 15.9 kN and 16.3 kN). Note that the manufacturer of the basalt textiles reports a tensile strength equal to 66 kN/m, which yields a tensile strength value for a 200 mm wide strip equal to  $66 \cdot (200/1000) = 13.2$  kN, slightly below the experimentally obtained value of 15.5 kN.

### **Experimental Setup and Procedure**

All specimens were subjected to monotonic tensile loading. Series A specimens were tested using a universal testing machine with a 250 kN MTS actuator, whereas Series B specimens were tested using a 500 kN MTS actuator fixed on the top beam of a stiff steel frame. In all cases the load was applied at a displacement rate of 0.01 mm/sec.

In the test setup for Series A, each specimen was suspended from the top grip of the testing machine through a steel ring, which was bolted to a threaded rod placed in the center of the concrete prism during casting. The load was applied at the two bearing surfaces of the wallette through a custom made clamping system (Fig. 7a). This system comprised a pair of two steel plates (one placed at the bearing surface and the other placed at the bottom of a stiff steel tube) and a pair of threaded rods. The steel tube at the bottom of the specimen was attached to the bottom grip of the machine through a steel ring, thus allowing the rotation of the specimen. As the concrete prism was allowed to rotate freely in 3D the setup was self-centering, thus resulting in perfectly symmetrical loading of the anchors on the two sides of the specimen.

In addition to the internal LVDT (Linear Variable Differential Transformer) of the actuator, displacement measurements were provided by external LVDTs measuring: (a) the relative displacement between the concrete prism and a fixed reference point (Fig. 7b,c), in order to monitor any deformation of the concrete prism; and (b) the relative displacement between the brick wallette (at a point near the masonry-concrete interface) and the same reference point (Fig. 7b).

In the test setup for Series B, the reinforced concrete prism was fixed at the base of the stiff steel frame through a pair of stiff steel tubes, placed on top of the two flanges of the prism, and two pairs of threaded rods (Fig. 7d). The load was applied at the two bearing surfaces of the wallette through a custom made clamping system, similar to the one used in the test setup of Series A. The swivel of the actuator was attached to a steel plate welded at the center of a steel tube. The actuator was placed at the centerline of the specimen, providing symmetrical loading conditions. Because of the 3D hinge of the actuator, possible geometrical eccentricities or eccentricities induced to the system due to local damage during the experiment, did not affect the nature of loading (pure tensile). Two external LVDTs were mounted to the bottom of the bearing surfaces to monitor the in-plane rotation of the brick wallette.

## Experimental Results

### Series A

Figure 8a shows typical load versus actuator displacement curves for specimens in Series A. All specimens in this series failed when one anchor ruptured at the concrete-wallette interface (Fig. 10a), resulting in a sudden load drop. Mean values of the maximum loads for specimens A\_W400-D150<sub>i</sub> (i=a,b), A\_W400-D75<sub>i</sub> (i=a,b) and A\_W600-D75<sub>i</sub> (i=a,b) were 15.05 kN, 13.95 kN and 16.65 kN; all values for the six specimens tested are given in Table 1.

An interesting aspect of the behavior in specimens of Series A may be seen in Fig. 8b, which shows load versus displacement plots for a typical test of the series, that corresponding to specimen A\_W400-D150a (the results for all other specimens were quite similar). The figure illustrates the opening of a “crack”, that is the creation of a gap, at the concrete-wallette interface, at a load approximately equal to 7 kN. Thereafter this gap increases almost linearly, confirming the elastic response of the anchors crossing the interface.

## **Series B**

The load versus displacement (average value of two externally mounted LVDTs) curves recorded for all specimens in Series B are shown in Fig. 9. The curves are grouped on the basis of the type of textile (“heavy”, H or “light”, L) and the number of layers (1 or 2). All curves are characterized by an initial linear branch, followed by a second ascending branch of gradually decreasing slope. The point where the initial branch meets the second one indicates “cracking” at the concrete-wallette interface and creation of a gap. Failure modes and failure loads for all tests in Series B are summarized in Table 1.

The control specimen of the group that received the heavy textile (specimen B\_H1\_CON) failed at an ultimate load of 33.5 kN. In this specimen the crack formation at the concrete-wallette interface was followed by the formation of some minor cracks in the TRM at the location of bed joints. Failure was controlled by the sudden rupture of the textile on both sides of the specimen exactly at the level of the concrete-wallette interface. In the same group, specimens B\_H1\_W400-L350 and B\_H1\_W400-L350<sub>in</sub> failed at 36.6 kN and 39.8 kN, respectively. In these specimens formation of minor cracking at the concrete-wallette interface was followed by the formation of a major crack on each side of the specimen at the position where the fanned part of the anchor terminated in the masonry; these major cracks indicated premature debonding of the anchor at the end of its fanned part. Both B\_H1\_W400-L350 and B\_H1\_W400-L350<sub>in</sub> failed when the anchor on one side debonded fully with respect to the TRM, as illustrated in Fig. 10b. Finally, specimen B\_H1\_W400-L500 of the same group, with greater length of the fanned part of the anchor, failed at a load equal to 50.8 kN. In this specimen the formation of minor cracking at the concrete-wallette interface was followed by the formation of minor cracking in the TRM at the location of some bed joints. The specimen failed when the anchor on one side debonded in the region between the

concrete-wallette interface and the flange of the concrete slab, that is on top of the concrete, and then ruptured suddenly as a result of the force released due to debonding (Fig. 10c).

The control specimens of the groups that received the light textile (specimens B\_L1\_CON and B\_L2\_CON) failed at an ultimate load of 23.9 kN and 48.3 kN, respectively. The behavior of these specimens in terms of crack formation and failure mode was similar to the case of specimen B\_H1\_CON (with the heavy textile) described above: failure was controlled by rupture of the textile at the concrete-wallette interface (Fig. 10d). A minor difference in specimen B\_L1\_CON was that rupture of the fibers in the textile was gradual (Fig. 9b), as a result of partial debonding of the rovings in the direction of loading. Specimens B\_L1\_W400-L350 and B\_L2\_W400-L350, with anchors that shaped a fan with a length of 350 mm, failed at an ultimate load of 38.3 kN and 68.7 kN, respectively. Specimens B\_L1\_W400-L500 and B\_L2\_W400-L500, with longer fanned parts in the anchors, reached a maximum load of 37.8 kN and 71.8 kN, respectively. The behavior of all these four specimens in terms of crack formation and failure mode was similar to the case of specimen B\_H1\_W400-L500 (with the heavy textile) described above: failure was controlled by anchor debonding through the mortar of the TRM system, in the region between the concrete-wallette interface and the flange of the concrete slab, followed by rupture of the anchor. A minor difference in specimen B\_L1\_W400\_L350 was that rupture of the anchor was gradual, as a result of partial debonding of the rovings in the direction of loading. Note that the large displacements recorded for specimen B\_L2\_W400-L350 (Fig. 9c) do not necessarily reflect more ductile behavior, but rather some unexpected local damage of the masonry near the two loading plates supporting the threaded rods. Specimens B\_L1\_W600-L500 and B\_L2\_W600-L500, with 50% heavier anchors, reached a maximum load of 50.3 kN and 63.7 kN, respectively. As in some of the previous cases, B\_L1\_W600-L500 failed when the anchor on one side debonded (through the mortar of the TRM system) in the region between the concrete-wallette interface and the flange of the concrete slab, that is on top of the concrete,

and then ruptured suddenly as a result of the force released due to debonding (Fig. 10e). Specimen B\_L2\_W600-L500 failed prematurely, due to local crushing of the masonry in contact with the bearing surfaces of the loading plates, hence its failure load may only be taken as a lower bound of that corresponding to the capacity of the anchored TRM.

Specimen B\_L1\_W400-L500<sub>eql</sub> deserves special attention, as it was added to the group of Series B on the basis of the observation that failure of the anchors in most cases was the result of debonding (through the mortar of the TRM system) in their length over the concrete, beyond the concrete-wallete interface. This debonding released suddenly substantial tensile forces in the straight part of the anchors (inside the concrete), which ruptured prematurely, as a result of stress concentrations near the bent region of the fibers. The whole idea behind specimen B\_L1\_W400-L500<sub>eql</sub> was to anchor the same amount of anchor fibers beyond the concrete-wallete interface not through the creation of a fan but in a straight configuration, which could be more effective in terms of debonding. This was confirmed by the test result for this specimen, which failed at a load of 47.9 kN due to rupture of the fibers at the concrete-wallete interface.

## Discussion

### Series A

The results from all tests are summarized in Table 1 and in a convenient graphical form in Fig. 11. In this figure, the values of maximum loads sustained by specimens in Series A (average values from two identical specimens) indicate that a reduction in the anchorage depth inside the concrete from 150 mm (A\_W400-D150) to 75 mm (A\_W400-D75) led only to a marginal reduction of the maximum load (by 7%, which may be considered as statistical error) because the failure mode (rupture of the anchors) remained unchanged. Moreover, comparison of the results for specimens A\_W400-D75 and A\_W600-75 indicates that an

increase in the quantity of fibers by 50%, for the same anchorage length of 75 mm, increased the failure load by approximately 19%, without affecting the failure mode.

Assuming perfectly symmetrical loading, the total load carried by each specimen divided by two gives the force carried by each anchor. This force is 7.53 kN, 6.98 kN and 8.33 kN in specimens A\_W400-D150, A\_W400-D75 and A\_W600-D75, respectively. If we recall that the experimentally obtained tensile strength of straight fibers in a 200 mm wide basalt textile is 15.5 kN and multiply this force by  $W/200$ , where  $W$  is the width of the anchor textile (in mm) in each specimen, we can estimate the tensile strength of the anchor assuming straight fibers subjected to tension. This force equals  $15.5 \cdot (400/200) = 31$  kN and  $15.5 \cdot (600/200) = 46.5$  kN for each anchor in specimens A\_W400-D150 or A\_W400-D75 and A\_W600-D75, respectively. Hence the effectiveness of each anchor, defined here by the ratio of maximum force carried by the anchor divided by tensile strength of fibers in a straight configuration, equals  $7.53/31 = 24\%$ ,  $6.98/31 = 23\%$  and  $8.33/46.5 = 18\%$  for the three specimens mentioned above, respectively. These low values are not surprising, as most of the fibers in the anchors develop stress concentrations at the concrete-wallette interface, where they are bent sharply before entering the hole inside the concrete.

### **Series B**

Assuming perfectly symmetrical loading of the textiles on both sides of the specimens, one layer of the heavy textile ( $610 \text{ g/m}^2$ ) in B\_H1\_CON resisted a force of  $33.5/2 = 16.75$  kN (see Fig. 11), whereas one layer of the light textile ( $405 \text{ g/m}^2$ ) in B\_L1\_CON resisted a force of  $23.9/2 = 11.95$  kN. Note that the ratio  $16.75/11.95 = 1.4$  is not too different from the ratio of  $610/405 = 1.5$ , hence the textiles in these two control specimens carried forces (nearly) proportional to the volume of fibers crossing the concrete-wallette interface. The same conclusion is valid by comparing specimens B\_L1\_CON with B\_L2\_CON, which had one and two layers, respectively, of the same (light) textile on each side. The two textile layers in

B\_L2\_CON resisted a force of  $48.3/2 = 24.15$  kN, which is nearly double the 11.95 kN resisted by one layer in B\_L1\_CON. The conclusion here is that all control specimens carried forces nearly proportional to the volume of fibers crossing the concrete-wallette interface.

As far as the contribution of anchors to the capacity of the specimens is concerned, Fig. 11 illustrates that in all specimens of Series B, except for B\_H1\_W400-L350 and B\_H1\_W400-L350<sub>in</sub>, the anchors (one per side) substantially increased the capacity of tensile force transfer between the brick wallette and the concrete prism. Anchors in the two aforementioned specimens debonded prematurely, while contributing only  $3.1/2 = 1.55$  kN and  $6.3/2 = 3.15$  kN each, in the strength of specimens B\_H1\_W400-L350 and B\_H1\_W400-350<sub>in</sub>, respectively. Their poor performance (early debonding) is attributed to the combination of a relatively short bond length in the masonry and the fact that they were bonded on top of heavy textile, which, when tensioned, produced high interlaminar shear stresses at the interface between the fanned part of the anchors and the textile. Each anchor in B\_H1\_W400-L500, the third specimen in the group of those with the heavy textile, sustained a force equal to  $17.3/2 = 8.65$  kN (Fig. 11), well above the forces carried by B\_H1\_W400-L350 and B\_H1\_W400-350<sub>in</sub>, which, as discussed above, failed by debonding in the masonry.

The next two specimens, B\_L1\_W400-L350 and B\_L1\_W400-L500, behaved similarly to B\_H1\_W400-L500: their failure was due to debonding of the anchors through the mortar of the TRM system, in their part covering the concrete, followed by anchor rupture. This explains why their different anchor bond lengths in the masonry (350 mm and 500 mm) did not affect the failure loads. Each anchor in these two specimens, B\_L1\_W400-L350 and B\_L1\_W400-L500, resisted  $14.4/2 = 7.2$  kN and  $13.9/2 = 6.95$  kN, respectively, values not too different from the 8.65 kN corresponding to B\_H1\_W400-L500. Notably, these three values of forces are in very good agreement with those carried by identical anchors in specimens A\_W400-D150 and A\_W400-D75 of Series A, where failure was due to anchor rupture.

A comparison between heavy and light anchors can be carried out calculating the force undertaken by each heavy anchor in specimen B\_L1\_W600-L500. This force equals  $26.4/2 = 13.2$  kN, which is about 85% higher than the average force corresponding to the lighter anchors in specimens B\_L1\_W400-L350 (7.2 kN) and B\_L1\_W400-L500 (6.95 kN). It is not surprising here that heavier anchors carry higher forces. The relationship between anchor fiber volume and anchor capacity is not linear, a fact which may be attributed to the complexity of the failure mechanism (anchor debonding in the region over the concrete followed by anchor rupture).

As in the case of specimens B\_L1\_W400-L350 and B\_L1\_W400-L500 (with one layer of textile on each side), the forces carried by each anchor in specimens B\_L2\_W400-L350 and B\_L2\_W400-L500 (with two layers of textile on each side) are not too different (their values are  $20.4/2 = 10.2$  kN and 11.75 kN, respectively). Here, too, failure was due to debonding of the anchors through the mortar of the TRM system, in their part covering the concrete, followed by anchor rupture, so that different anchor bond lengths in the masonry (350 mm and 500 mm) did not affect the failure load. However, anchor forces for the case of two textile layers are higher than those in the case of one layer, owing to the fact that placement of a single anchor in between two layers of the textile improves bond conditions (of the anchor), thereby delaying debonding. This increase in anchor effectiveness may be estimated by comparing anchor forces for specimens B\_L1\_W400-L350 and B\_L2\_W400-L350 (7.2 kN versus 10.2 kN), as well as for specimens B\_L1\_W400-L500 and B\_L2\_W400-L500 (6.95 kN versus 11.75 kN). On average, the improvement is about 55%.

As mentioned in the previous section, Specimen B\_L1\_W400-L500<sub>eql</sub> deserves special mention. In this specimen, anchorage of the textile at the concrete-wallete interface was improved with an extra patch of textile on each side, identical to that used to make the spike anchors. As given in Fig. 11, each of these patches carried a load of  $24/2 = 12$  kN, which is about 70% higher than that carried by the anchors in specimen B\_L1\_W400-L500. It is

confirmed that fibers crossing the concrete-wallette interface are more effective if placed “undisturbed”, that is straight (and parallel to tensile stresses), than in the form of a fan, which results in substantial stress concentrations in their bent part. However, this conclusion should be treated with caution, as it may not be valid in the case of geometries other than those used in the present study, e.g. when the available bond length on concrete is shorter, in which case the embedment of anchors inside holes through the concrete will be unavoidable.

## Conclusions

This paper presents a study on the development and testing of new textile-based anchors used to transfer tensile forces in models made of masonry wallettes and reinforced concrete prisms, simulating the connection between masonry infills and concrete frames through the use of textile-reinforced mortars (TRM). The experimental investigation involved specimens categorized in two groups, each one representing different boundary conditions between masonry and concrete. A general conclusion is that the anchors developed in this study enable the transfer of substantial tensile forces between masonry and concrete. More conclusions are summarized below for each of the two groups of specimens tested.

(a) If the thickness of the infill is less than the width of the concrete member:

- The spike anchors developed in this study fail by rupture in their bent part at the masonry-concrete interface, when tensile forces carried by them are about 20-25% of the uniaxial strength of straight fibers.
- Increasing the quantity of fibers in the anchors results in non-proportional increase of forces carried by them.

(b) If the thickness of the infill is equal to the width of the concrete member:

- Substantial tensile forces are transferred across the masonry-concrete interface even if no anchors are used, due the extension of the TRM over the concrete. If failure is controlled

by rupture of the TRM, these forces are nearly proportional to the quantity of fibers in the textile crossing the interface.

- The addition of anchors increases the tensile resistance of the interface even further, due to the contribution of the extra fibers in the anchors; this increase is non-proportional to the volume of fibers in the anchors.
- The typical failure mode of anchors involves debonding through the mortar of the TRM system, in their part over the concrete, followed by rupture of the fibers in their bent part. This failure mode was avoided only when the anchors were combined with heavy textiles, in which case they debonded prematurely in their part over the masonry.
- Anchors placed between two layers of textiles are more effective, by about 50%, than those placed on top of a single layer, due to improved bond conditions.

Considering that the textile-based anchors are new custom-made materials, tested for the first time in this experimental program, the results of this study should be considered as rather preliminary. Future research should be directed towards providing a better understanding of problem parameters including the bond length of TRM over the concrete surface, the angle of the shaped fan and the effect of cyclic loading.

## **Acknowledgements**

Partial support to this research has been provided by the European Union (European Social Fund – ESF) and Greek national funds through the Operational Program “Education and Lifelong Learning” of the National Strategic Reference Framework (NSRF) – Research Funding Program THALES - Investing in knowledge society through the European Social Fund. The authors wish to thank Assist. Prof. C. Papanicolaou for her advice and the students N. Karathanasopoulos and L. Panoutsopoulou for their assistance in the experimental program.

## References

- Almousallam, T. H., and Al-Salloum, Y. A. (2007). "Behavior of FRP strengthened infill walls under in-plane seismic loading." *J. Comp. Constr.*, 11(3), 308-318.
- Altin, S., Anil, Ö., Kara, E. M. and Kaya, M. (2008). "An experimental study on strengthening of masonry infilled RC frames using diagonal CFRP strips." *Composites: Part B*, 39, 680-693.
- Altin, S., Anil, Ö., Kopruman, Y., and Belgin, C. (2010). "Strengthening masonry infill walls with reinforced plaster." *Proc. ICE - Structures and Buildings*, 163(5), 331-342.
- Al-Salloum, Y. A., Siddiqui, N. A., Elsanadedy, H. M., Abadel, A.A., and Aqel, M. A. (2011). "Textile-reinforced mortar versus FRP as strengthening material for seismically deficient RC beam-column joints." *J. Comp. Constr.*, 15(6), 920-933.
- Al-Salloum, Y. A., Elsanadedy, H. M., Alsayed, S. H., and Iqbal, R. A. (2012). "Experimental and numerical study for the shear strengthening of reinforced concrete beams using textile reinforced mortar." *J. Comp. Constr.*, 16(1), 74-90.
- Akin, E., Ozcebe, G., and Ersoy, U. (2009). "Strengthening of brick infilled RC frames with CFRP sheets." In *Seismic Risk Assessment and Retrofitting*, Ilki et al. eds., 367-386.
- Blanksvärd, T., Täljsten, B., and Carolin, A. (2009). "Shear strengthening of concrete structures with the use of mineral-based composites." *J. Comp. Constr.*, 13(1), 25-34.
- Bournas, D., Lontou, P., Papanicolaou, C. G. and Triantafillou, T. C. (2007). "Textile-reinforced mortar (TRM) versus FRP confinement in reinforced concrete columns." *ACI Struct. J.*, 104(6), 740-748.
- Bournas, D., Triantafillou, T. C., Zygouris, K., and Stavropoulos, F. (2009). "Textile-reinforced mortar versus FRP jacketing in seismic retrofitting of RC columns with continuous or lap-spliced deformed bars." *J. Comp. Constr.*, 13(5), 360-371.
- Bournas, D., and Triantafillou, T. C. (2011). "Bar buckling in RC columns confined with composite materials." *J. Comp. Constr.*, 15(3), 393-403.
- Bousias, S., Spathis, A. L., Fardis, M., Triantafillou, T. C., and Papanicolaou, C. (2007). "Pseudodynamic tests of non-seismically designed RC structures retrofitted with textile-reinforced mortar." *Proc., 8th Int. Symp. on Fiber Reinforced Polymer Reinforcement for Concrete Structures (FRPRCS-8)*, Patras, Greece.

- Brückner, A., Ortlepp, R., and Curbach, M. (2008). "Anchoring of shear strengthening for T-beams made of textile reinforced concrete (TRC)." *Mater. Struct.*, 41(2), 407-418.
- Elsanadedy, H. M., Almusallam, T. H., Alsayed, S. H., and Al-Salloum, Y. A. (2013). "Flexural strengthening of RC beams using textile reinforced mortar – Experimental and numerical study." *Comp. Struct.*, 97, 40-55.
- EN 1015-11 (1993). *Methods of test for mortar for masonry – Part 11: Determination of flexural and compressive strength of hardened mortar*, European Committee for Standardization, Brussels.
- Erdem, I., Akyuz, U., Ersoy, U., and Ozcebe, G. (2006). "An experimental study on two different strengthening techniques for RC frames." *Engrg. Struct.*, 28, 1843-1851.
- Erol, G., Karadogan, H. F., and Cili, F. (2008). "Seismic strengthening of infilled RC frames by CFRP." *Proc. 14<sup>th</sup> World Conf. Earthq. Engrg.*, Beijing, China.
- Harajli, M., ElKhatib, H., and San-Jose, J. (2010). "Static and cyclic out-of-plane response of masonry walls strengthened using textile-mortar system." *J. Mater. Civ. Eng.*, 22(11), 1171-1180.
- Koutas, L., and Triantafillou, T. C. (2013). "Use of anchors in shear strengthening of reinforced concrete T-beams with FRP." *J. Comp. Constr.*, 17(1), 101-107.
- Kyriakides, M. A., and Billington, S. L. (2008) "Seismic retrofit of masonry-infilled non-ductile reinforced concrete frames using sprayable ductile fiber-reinforced cementitious composites." *Proc. 14<sup>th</sup> World Conf. Earthq. Engrg.*, Beijing, China.
- Nateghi-Elahi, F., and Dehghani, A. (2008). "Experimental behavior of brick-infilled concrete frames strengthened by CFRP with improved attaching technique." *Proc. 14<sup>th</sup> World Conf. Earthq. Engrg.*, Beijing, China.
- Ozcebe, G., Ersoy, U., Tankut, T., Erduran, E., Keskin, O., and Mertol. C. (2003). "Strengthening of brick-infilled RC frames with CFRP" *TUBITAK Structural Engineering Research Unit Report No. 2003-1*, METU, Ankara, Turkey.
- Ozden, S., Akguzel, U., and Ozturan T. (2011). "Seismic strengthening of infilled reinforced concrete frames with composite materials" *ACI Struct. J.*, 108(4), 414-422.
- Papanicolaou, C. G., Triantafillou, T. C., Karlos, K., and Papathanasiou, M. (2007). "Textile-reinforced mortar (TRM) versus FRP as strengthening material of URM walls: in-plane cyclic loading." *Mater. Struct.*, 40(10), 1081-1097.

- [Papanicolaou, C. G., Triantafillou, T. C., Papathanasiou, M., and Karlos, K. \(2008\). "Textile-reinforced mortar \(TRM\) versus FRP as strengthening material of URM walls: out-of-plane cyclic loading." \*Mater. Struct.\*, 41\(1\), 143-157.](#)
- Papanicolaou, C. G., Triantafillou, T. C., Papantoniou, I., and Balioukos, C. (2009). "Strengthening of two-way slabs with textile reinforced mortars (TRM)." *Proc. 11<sup>th</sup> fib Symposium*, London, UK.
- [Parisi, F., Lignola, G. P., Augenti, N., Prota, A., and Manfredi, G. \(2011\). "Nonlinear behavior of a masonry subassembly before and after strengthening with inorganic matrix-grid composites." \*J. Comp. Constr.\*, 15\(5\), 821-32.](#)
- [Saatcioglu, M., Serrato, F., and Foo, S. \(2005\). "Seismic performance of masonry infill walls retrofitted with CFRP sheets." \*Proc. 7<sup>th</sup> Intern. Symp. Fiber-Reinforced Polymer Reinforcement for Concrete Structures \(FRPRCS-7\)\*, SP-230, New Orleans, USA.](#)
- [Sevil, T., Baran, M., Bilir, T., and Canbay, E. \(2011\). "Use of steel fiber reinforced mortar for seismic strengthening." \*Constr. Build. Mater.\*, 25, 892-899.](#)
- Triantafillou, T. C., Papanicolaou, C. G., Zissimopoulos, P., and Laourdekis, T. (2006). "Concrete confinement with textile-reinforced mortar jackets." *ACI Struct. J.*, 103(1), 28-37.
- [Triantafillou, T. C., and Papanicolaou, C. G. \(2006\). "Shear strengthening of reinforced concrete members with textile reinforced mortar \(TRM\) jackets." \*Mater. Struct.\*, 39\(1\), 93-103.](#)
- Triantafillou, T. C. (2007). "Textile-reinforced mortars (TRM) versus fibre-reinforced polymers (FRP) as strengthening and seismic retrofitting materials for reinforced concrete and masonry structures." *Proc. Intern. Conf. Advanced Composites in Construction (ACIC07)*, University of Bath, April 2-4.
- [Yuksel, E., Ilki, A., Erol, G., Demir, C., and Karadogan, H. F. \(2006\). "Seismic retrofitting of infilled reinforced concrete frames with CFRP composites." \*Proc. NATO Workshop: Advances in Earthquake Engineering for Urban Risk Reduction\*, Istanbul.](#)
- [Zhang, H. W., and Smith, S. T. \(2012\). "Influence of FRP anchor fan configuration and dowel angle on anchoring FRP plates." \*Composites: Part B\*, 43, 3516 -3527.](#)

## List of Figures

- Fig. 1 (a) TRM-strengthening of infill with different possible boundary conditions. (b) Schematic placement of anchors.
- Fig. 2 Geometry of specimens in (a) Series A and (b) Series B (dimensions in mm).
- Fig. 3 Schematic view of specimens tested.
- Fig. 4 Textiles used in this study: (a) Epoxy-coated E-glass with mesh size 10x10 mm; (b) elastomeric polymer-coated E-glass with mesh size 25x25 mm; (c) uncoated basalt textile with mesh size 25x25 mm.
- Fig. 5 Steps for the fabrication of a textile-based spike anchor: (a) Partial removal of transverse rovings; (b) cutting of fiber rovings in the transverse direction; (c) shaping of the anchor; (d) epoxy impregnation of tow of fibers at one end of the anchor; (e) epoxy impregnating of the textile in the fanned part; (f) ready-to-use textile-based anchor after curing of the epoxy.
- Fig. 6 Basic strengthening procedure steps: (a) application of mortar on the surfaces receiving TRM layers; (b) application of first textile layer; (c) impregnation of anchor dry fibers with epoxy adhesive; (d) bonding of the anchor fan over the first textile layer.
- Fig. 7 (a) Series A test setup; (b) front side instrumentation; (c) back side instrumentation; (d) Series B test setup.
- Fig. 8 (a) Selected load versus actuator displacement curves for specimens in Series A. (b) Calculation of gap opening at the concrete-wallette interface.
- Fig. 9 Load versus displacement curves of Series B specimens.
- Fig. 10 (a) Anchor rupture in a specimen of Series A at the concrete-wallette interface; (b) debonding of the anchor at the edge of the fan in specimen B\_H1\_W400-L350; (c) anchor debonding over the concrete and rupture in specimen B\_H1\_W400-L500; (d) rupture of fibers in B\_L2\_CON specimen; (e) anchor debonding (through the mortar

of the TRM system) over the concrete and rupture in specimen B\_L1\_W600-L500;

(f) anchor debonding over the concrete and rupture in specimen B\_L2\_W400-L500.

Fig. 11 Strength provided by the anchors in all specimens.

**Table 1.** Test Parameters and Summary of Test Results

Specimen index	Notation	Textile layers (per side), Type of textile	Anchor properties (per side)		Failure mode	Peak tensile force (kN)
			Width of textile (mm)	Length of the fanned part (mm)		
<b>Series A</b>						
1	A_W400-D150 <sub>a</sub>	1, Heavy (H)	400	350	AR <sup>1</sup>	15.3
2	A_W400-D150 <sub>b</sub>	1, H	400	350	AR	14.8
3	A_W400-D75 <sub>a</sub>	1, H	400	350	AR	14.8
4	A_W400-D75 <sub>b</sub>	1, H	400	350	AR	13.1
5	A_W600-D75 <sub>a</sub>	1, H	600	350	AR	14.7
6	A_W600-D75 <sub>b</sub>	1, H	600	350	AR	18.6
<b>Series B</b>						
7	B_H1_CON	1, H*	---	---	TR <sup>2</sup>	33.5
8	B_H1_W400-L350	1, H*	400	350	ADm <sup>3</sup>	36.6
9	B_H1_W400-L350 <sub>in</sub>	1, H*	400	350	ADm	39.8
10	B_H1_W400-L500	1, H	400	500	ADc <sup>4</sup> , AR	50.8
11	B_L1_CON	1, Light (L)	---	---	TR	23.9
12	B_L2_CON	2, L	---	---	TR	48.3
13	B_L1_W400-L350	1, L	400	350	ADc, AR	38.3
14	B_L2_W400-L350	2, L	400	350	ADc, AR	68.7
15	B_L1_W400-L500	1, L	400	500	ADc, AR	37.8
16	B_L2_W400-L500	2, L	400	500	ADc, AR	71.8
17	B_L1_W600-L500	1, L	600	500	ADc, AR	50.3
18	B_L2_W600-L500	2, L	600	500	BC <sup>5</sup>	63.7
19	B_L1_W400-L500 <sub>eq</sub>	1**, L	---	---	TR	47.9

\* Partial coverage of the wallette surface; \*\* an extra layer of basalt textile equivalent to a W400-L500 anchor was used; <sup>1</sup> anchor rupture; <sup>2</sup> textile rupture; <sup>3</sup> anchor debonding at the end of the fanned part in the masonry; <sup>4</sup> anchor debonding in the part over the concrete, between the concrete-wallette interface and the concrete slab; <sup>5</sup> brick crushing.

**Table 2.** 28-Day Compressive Strength of Concrete

Specimen index	Concrete strength $f_c$ (MPa)
1-6	44.4
7-10	38.0
11-19	28.5

**Table 3.** 28-Day Strength of Mortar used for Joints of Brick Wallettees

Specimen index	Compressive strength $f_m$ (MPa)	Flexural strength $f_{m,fl}$ (MPa)
1-6	23.6	5.6
7-10	9.4	2.1
11-19	6.1	1.6

**Table 4.** Properties of Textiles

	Epoxy-coated E-glass fiber	Elastomeric polymer-coated E-glass fiber	Uncoated basalt fiber (used in anchors)
Mesh size (mid-roving to mid-roving grid spacing)	10x10 mm	25x25 mm	25x25 mm
Net grid spacing	7 mm	21 mm	23 mm
Weight	610 g/m <sup>2</sup>	405 g/m <sup>2</sup>	192 g/m <sup>2</sup>
Tensile strength per running meter	147 kN/m *	115 kN/m **	66 kN/m **
Rupture strain	2.3 %	2.5 %	3.15 %
Modulus of elasticity	70 GPa	73 GPa	89 GPa
Fiber density	2.6 g/cm <sup>3</sup>	2.6 g/cm <sup>3</sup>	2.66 g/cm <sup>3</sup>

\* Calculated using nominal value of thickness (obtained from the equivalent smeared distribution of fibers); \*\* taken from data sheets of the manufacturer.

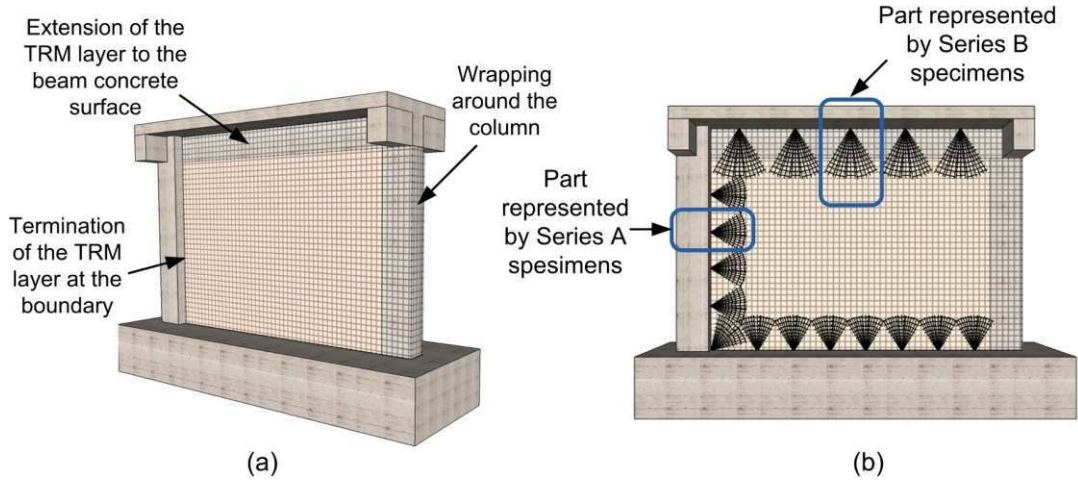


Fig. 1

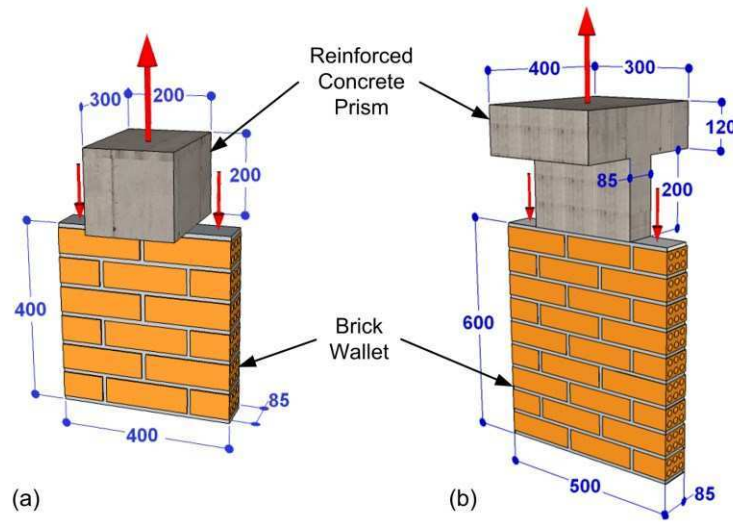


Fig. 2

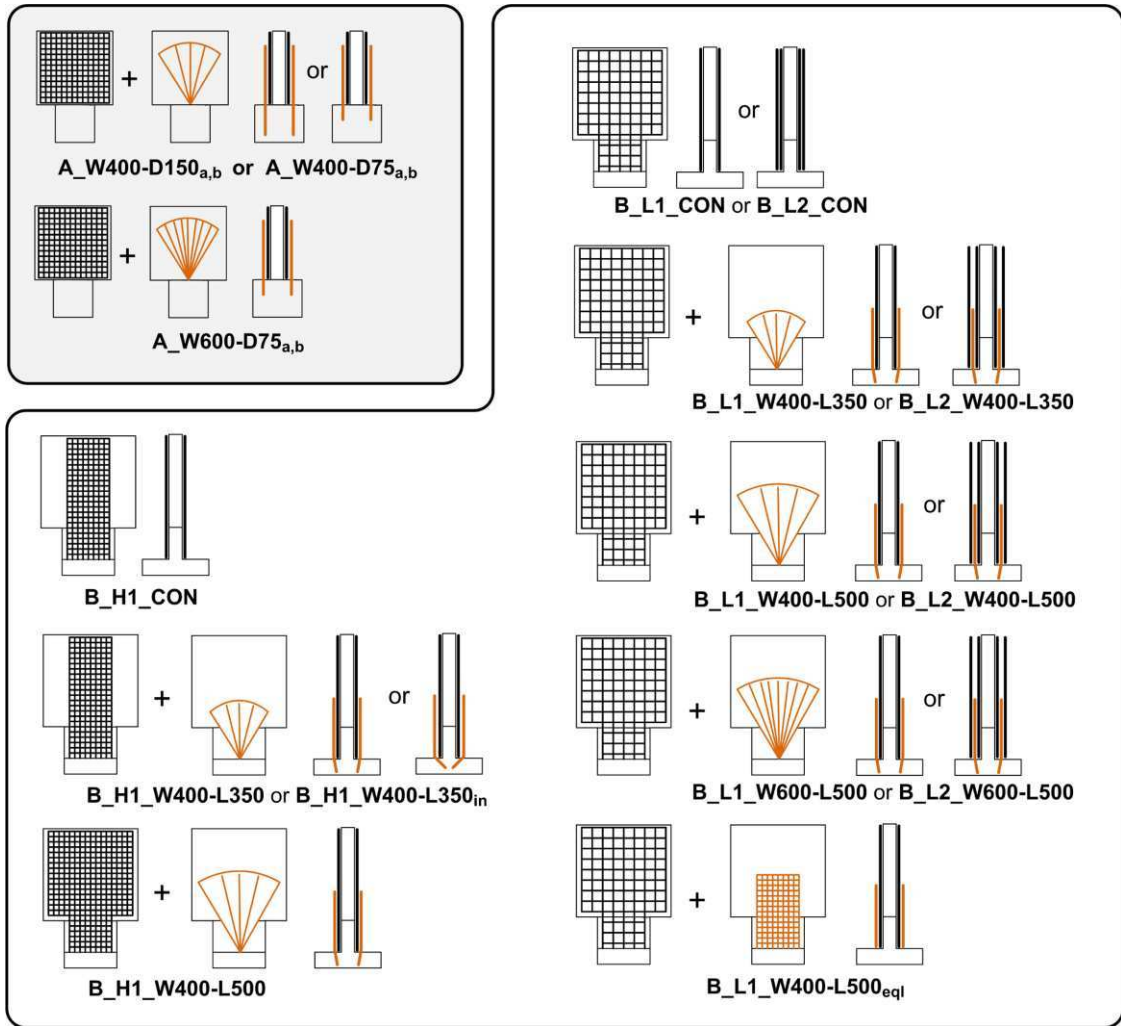


Fig. 3



Fig. 4

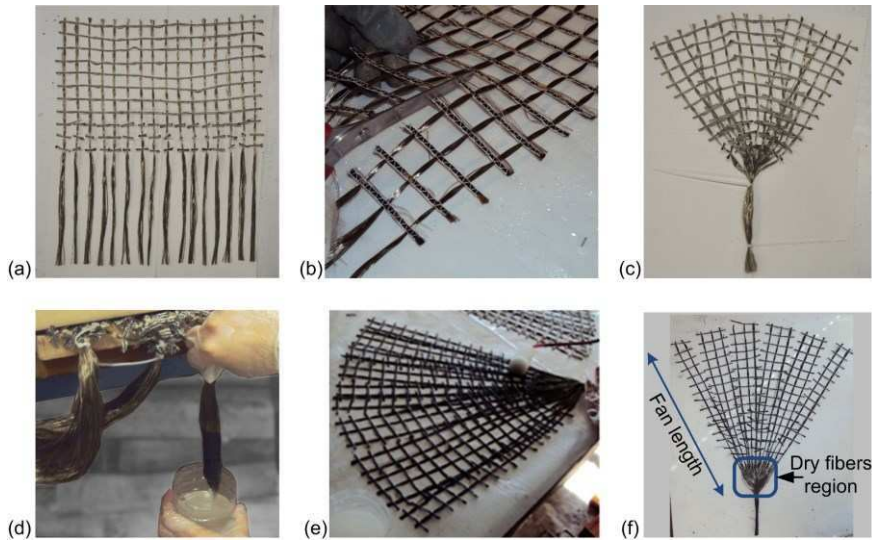


Fig. 5

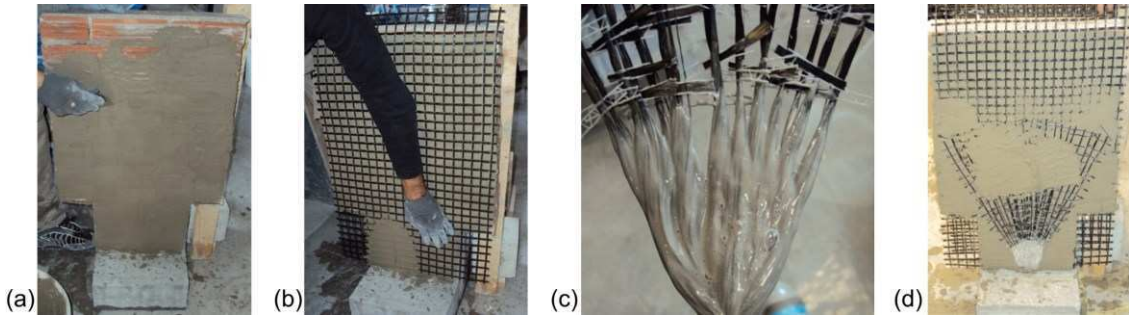


Fig. 6

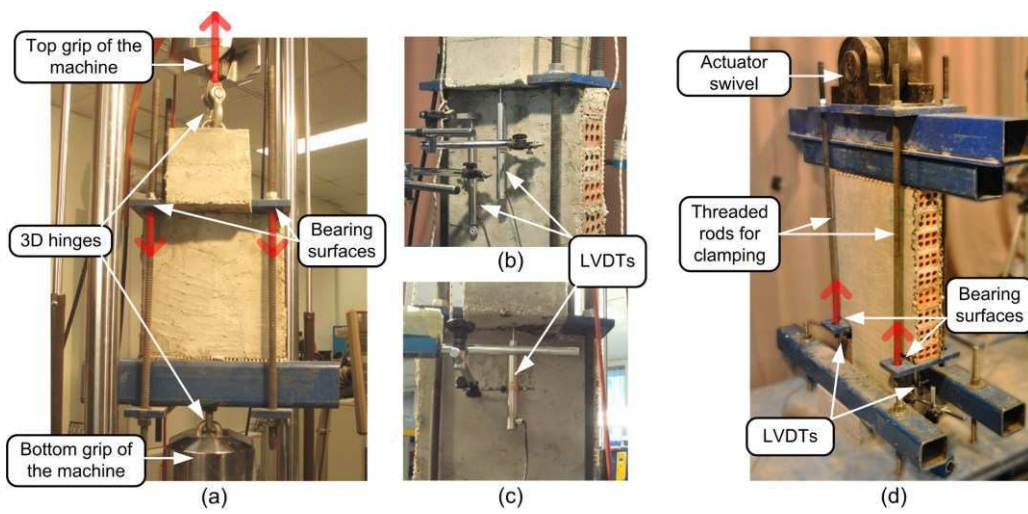


Fig. 7

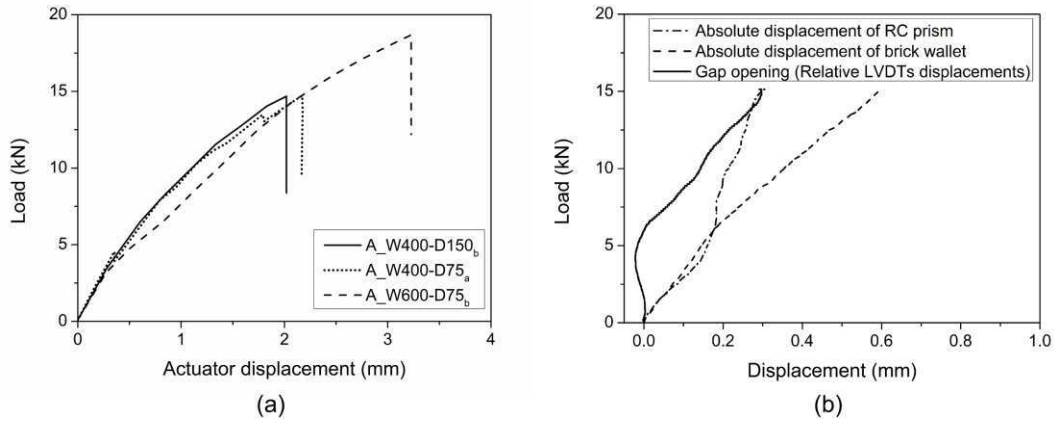


Fig. 8

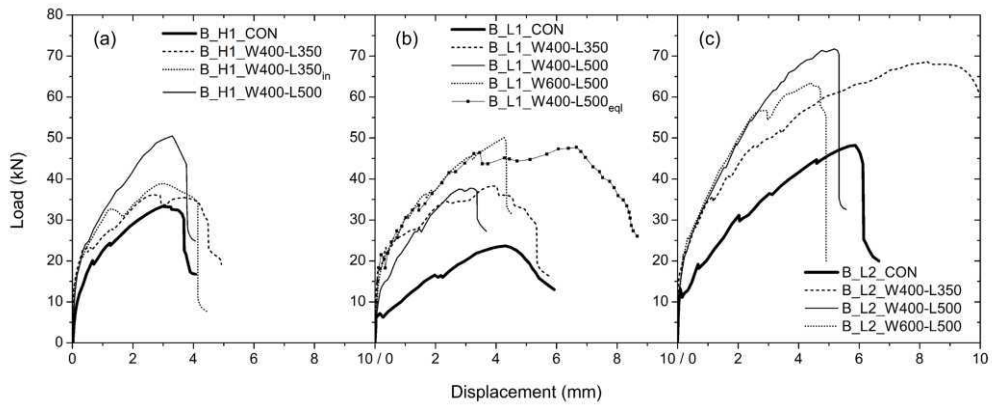


Fig. 9

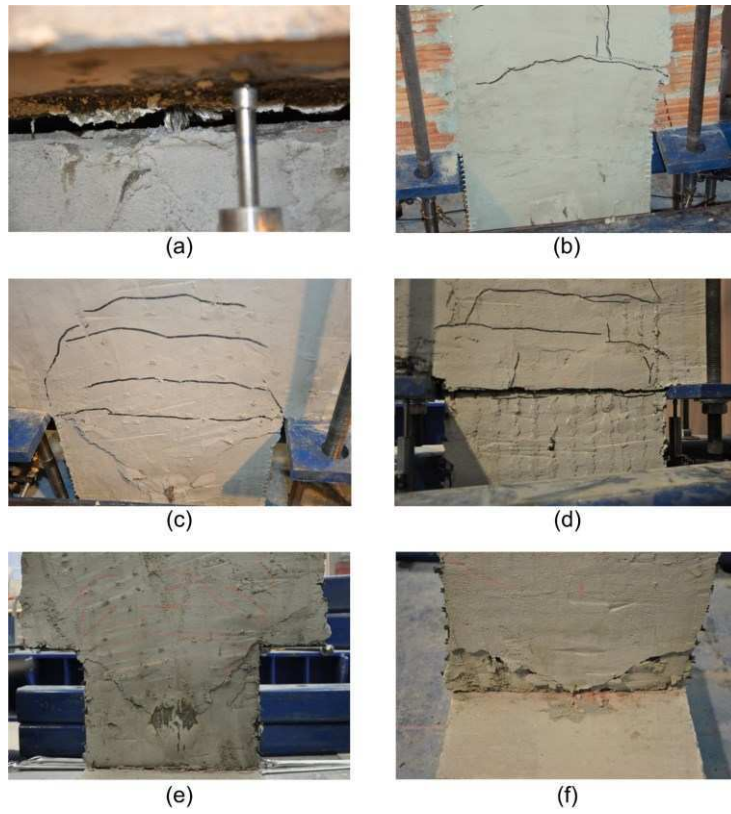


Fig. 10

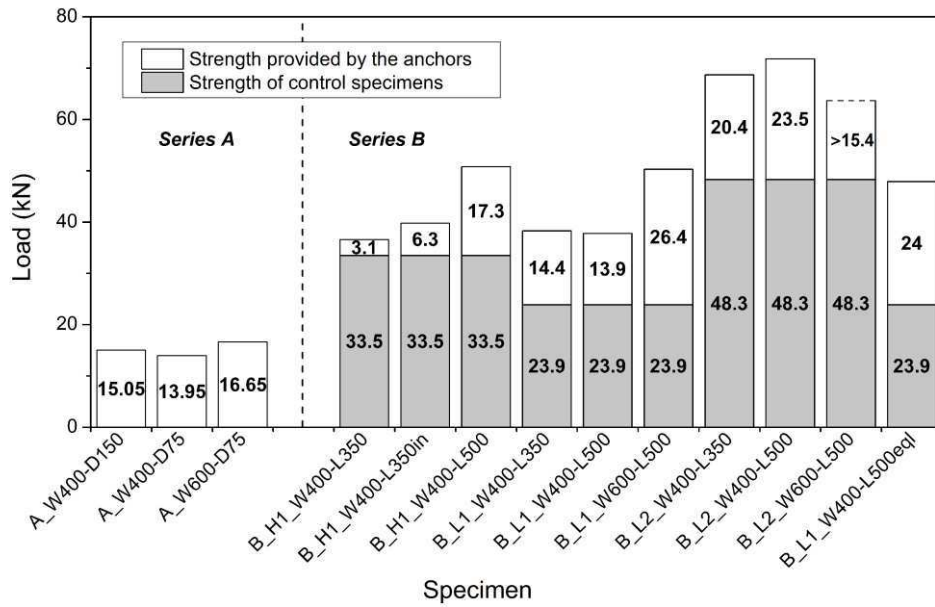


Fig. 11